Supporting Information

On the Role of Ligands in Atomically Precise Nanocluster-Catalyzed CO_2 Electrochemical Reduction

Site Li,[†,‡,1] Anantha Venkataraman Nagarajan, [§,1] Yingwei Li,[†] Douglas R. Kauffman,*[,‡] Giannis Mpourmpakis, *[,§] and Rongchao Jin*[,†]

† Department of Chemistry, Carnegie Mellon University, Pittsburgh, Pennsylvania 15213, USA

§ Department of Chemical Engineering, University of Pittsburgh, Pittsburgh, Pennsylvania 15261, United States

‡National Energy Technology Laboratory (NETL), United States Department of Energy, Pittsburgh, Pennsylvania, USA.

Experimental Details

Chemicals. All chemicals are commercially available and used with no further purification. Tetrachloroauric(III) acid ($HAuCl_4 \cdot 3H_2O$, 99.99% metal basis), sodium borohydride (99.99% trace metals basis), phenylethanethiol ($PhCH_2CH_2SH$, 98%), selenophenol (PhSeH, ≥99.9%), 1-Naphthalenethiol (99%), tetrahydrofuran (THF, HPLC grade, 99.9%), methanol (HPLC grade, 99.9%), dichloromethane (DCM, HPLC grade, 99.9%), 2-propanol (HPLC grade, 99.9%), Nafion 117 solution (~5% in a mixture of lower aliphatic alcohols and water) were purchased from Sigma-Aldrich. Tetraoctylammonium bromide (TOAB, 98%) was obtained from Fluka. XC-72 carbon black was bought from Cabot Corporation.

Synthesis of Au nanoclusters. phenylethanethiol protected Au_{25} were synthesized with our previously reported methods.[1] First, $HAuCl_4 \cdot 3H_2O$ (0.16 mmol, 62.0 mg) and TOAB (0.167 mmol, 91.2 mg) were mixed in 15 mL THF in a tri-neck flask under stirring for 5 min, followed by addition of $PhCH_2CH_2SH$ (0.8 mmol, 112 ìL). After 30 min, 1.5 mL aqueous $NaBH_4$ (1.6 mmol, 60 mg) solution was rapidly added into the mixture. The solution turned black immediately, indicating the reduction Au(I) to Au(0). The reaction was allowed to proceed for 8 hours. Finally, the solution was washed with methanol three times and the phenylethanethiol protected Au_{25} nanoclusters were extracted with dichloromethane. Naphthalenethiol protected

Au_{25} was obtained by ligand exchange from phenylethanethiol protected Au_{25}.[2] The synthesis of selenol protected Au_{25} is similar to that of phenylethanethiol protected Au_{25}.[3] But the selenophenol and $NaBH_4$ were reduced to 0.4 mmol and 0.3 mmol, respectively. During the reduction step, the selenophenol and $NaBH_4$ aqueous solution were added simultaneously.

Characterization. UV–vis spectra were collected on a Hewlett–Packard (HP) Agilent 8453 diode array spectrophotometer at room temperature. ^1H nuclear magnetic resonance spectroscopy (Bruker Avance 500 MHz) was used for detection of liquid products.

Electrochemical measurements. All electrochemical measurements were carried out in a custom two-compartment H-cell. CO_2 reduction was conducted using a SP150 (Biologic) electrochemical station. Glassy carbon was used as working electrode. Ag/AgCl electrode and a platinum wire electrode were used as the reference and counter electrodes, respectively. To prepare the catalytic sample, the as prepared Au_{25} nanoclusters were loaded on carbon black with a ratio of 10% wt. The catalytic ink was prepared by dispersing the catalytic sample in isopropyl alcohol (4 mg/ml) and sonicated for 30 min. After that, 5 ìL catalysts suspension and 5 ìL 0.2 wt% Nafion were dropped onto the glassy carbon electrode. 0.5 M $KHCO_3$ aqueous solution was used as electrolyte. Reaction products were quantified using a Perkin Elmer Clarus 600 gas chromatograph equipped with thermal conductivity and flame ionization detectors.

Computational Details

Electronic structure calculations were performed at the density functional theory (DFT) level. The exchange-correlation energy was accounted using the Perdrew-Burke-Ernzerhof (PBE)[4] functional. The energy of the core atoms was approximated using Goedecker, Teter, and Hutter (GTH) pseudopotentials[5]. The electronic wavefunctions of all atoms were described using the double-ζ plus polarization (DZVP) basis set[6] with a cutoff of 500 Ry as implemented in the computational package CP2K[7]. A non-periodic cell of dimensions 30 x 30 x 30 $Å^3$ was used to optimize all structures until forces between the atoms were less than 0.002 $eV \cdot A^{-1}$. The structure of the $[Au_{25}(SR)_{18}]^{1-}$ and $[Au_{25}(SeR)_{18}]^{1-}$ nanoclusters (R = $CH_2CH_2C_6H_5$ and C_6H_5 respectively), has been successfully characterized using single crystal XRD[8, 9]. The -R groups were replaced by

methyl (-CH_3) groups in all the DFT calculations. This approach reduces computational cost while accurately capturing trends in catalytic behavior of atomically precise gold nanoclusters[10-12]. Especially in our case, this approach is valid on addressing general catalytic trends at the S/Se-metal interface. Previous studies[12-14] have shown that in order to activate the Au_{25} nanocluster for CO_2 reduction, the -R group from the thiolate-protecting layer (surface) of the nanocluster must be released to expose active sites. The same concept is applied here, and the energy required to release the -R group is calculated as an electrochemical reduction step as follows:

$$\frac{1}{2}H_2 + [Au_{25}(XR)_{18}]^{1-} \rightarrow [Au_{25}X(XR)_{17}]^{1-} + HR \qquad (1)$$

In the above reaction, the -R group is removed to generate an exposed S or Se on the nanocluster surface, where *X* represents S or Se. The Gibbs free energy for all the systems was calculated using statistical thermodynamics, wherein the vibrational modes were calculated using the harmonic oscillator approximation.

Free energies of COOH* and CO* adsorption were calculated per equation 1:

$$\Delta G = \Delta E + \Delta ZPE + \int C_P dT - TS \qquad (2)$$

Where ZPE represents the Zero Point Energy, Cp (heat capacity), and S (entropy) terms and E, the electronic energy of each system. The vibrational modes of the adsorbate alone were considered into the free energy calculations. According to the PBE functional, gas phase corrections to the CO_2, CO, H_2 and H_2O molecules were applied as per the approach of Peterson *et al*[15]. Each electrochemical step involves the transfer of a proton-electron pair. The computational hydrogen electrode was used to account for the energy of this proton-electron pair where $G(H^+ + e^-) = ½\ G(H_{2(g)})$[15]. In order to include the effect of an applied potential 'U' for an electrochemical step, an additional 'neU' term was added to the Gibbs free energy of that step, where U is the applied potential, n is the number of electrons transferred and e is an elementary positive charge. The energetics are reported at 0 V against the reversible hydrogen electrode (RHE).

Table S1. Bader charge on sulfur/selenium atom on each Au_{25} nanocluster system upon -R removal

Nanocluster	**Bader charge (e) on sulfur/selenium**
Sulfur-Au_{25}	-0.31
Selenium-Au_{25}	-0.20

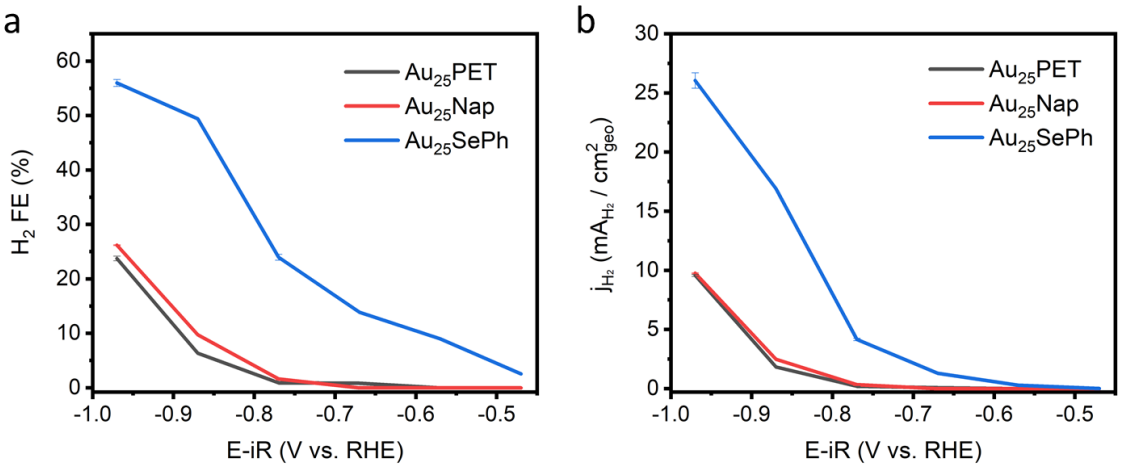

Figure S1. Electrocatalytic performance of Au_{25} nanoclusters. (a) Faradaic Efficiency (FE) for H_2 production and (b) H_2 partial current density.

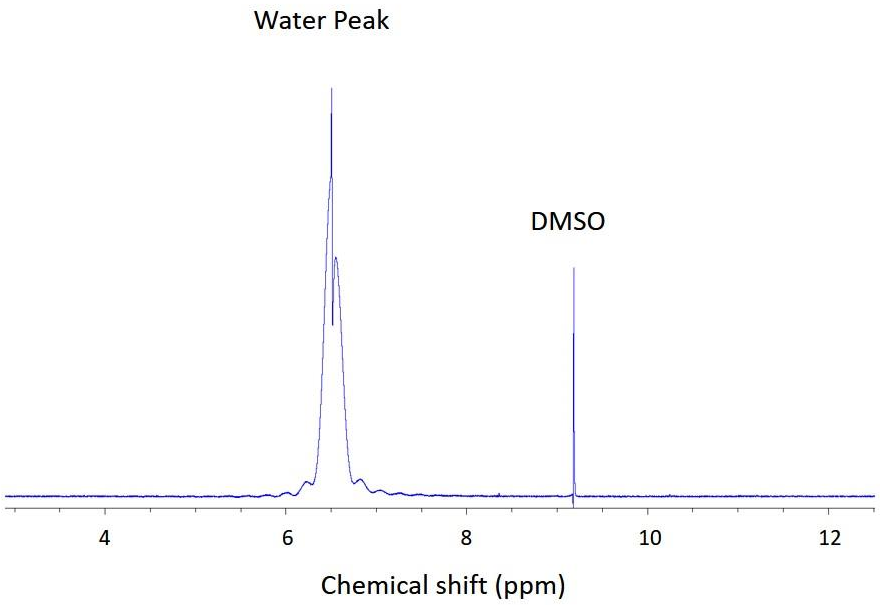

Figure S2. Typical ^{1}H nuclear magnetic resonance (NMR) spectrum of electrolyte after reaction. No liquid product of CO_2RR was found.

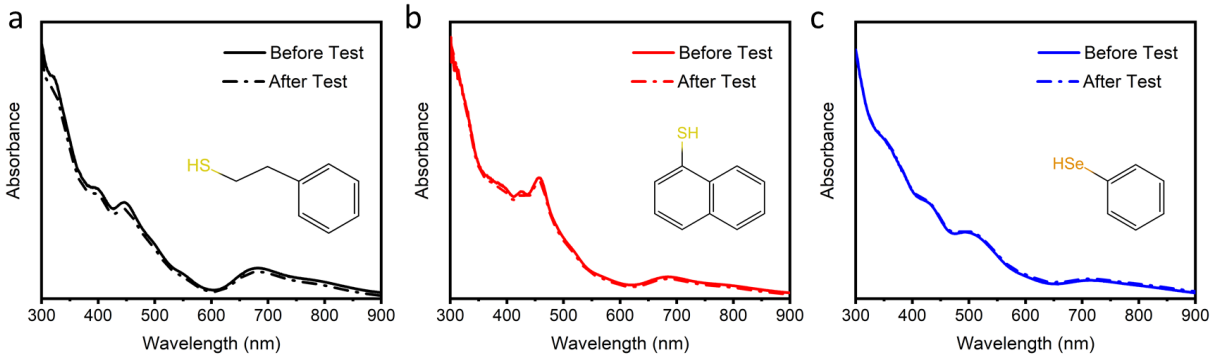

Figure S3. UV-vis spectroscopic tests of stability of the three Au_{25} nanoclusters at -0.8 V for 10 min (spectra before/after the CO2RR)

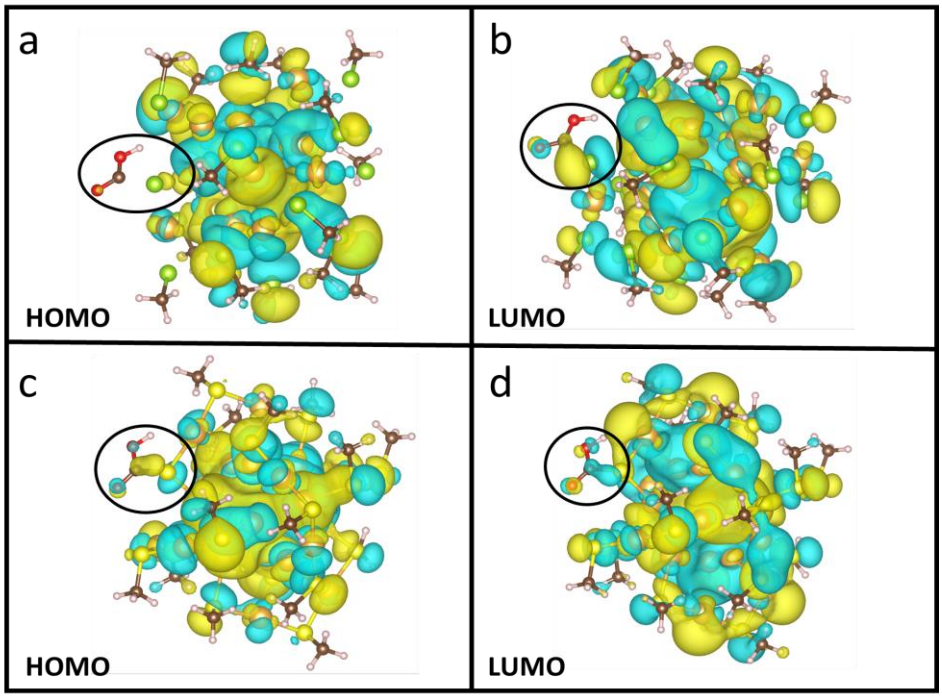

Figure S4. The highest occupied molecular orbital (HOMO) and lowest unoccupied molecular orbital (LUMO) of the Au_{25} nanoclusters upon COOH adsorption on the (a, b) selenium active site and (c, d) sulfur active site respectively. Black circle indicates site of adsorption, enclosing the S/Se atom and the COOH intermediate.

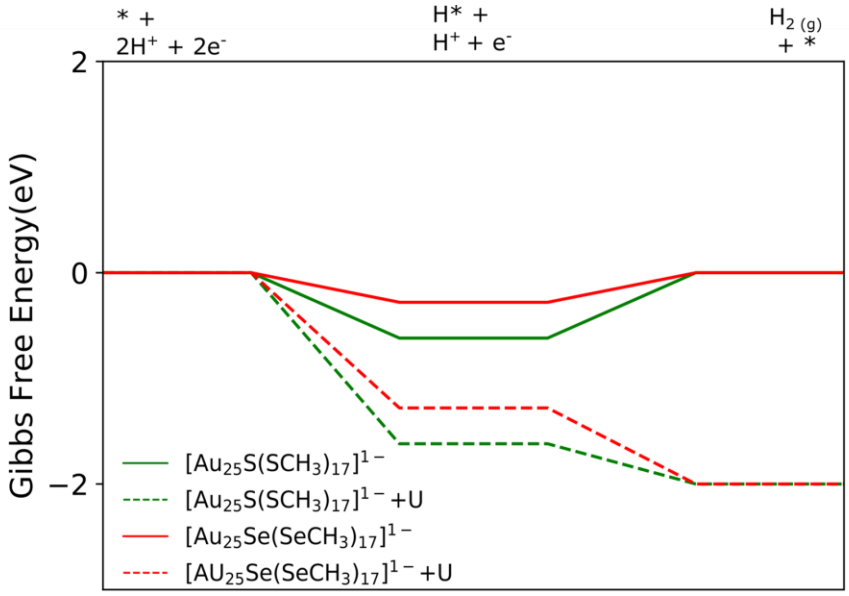

Figure S5. HER pathway on sulfur-based (green) and selenium-based (red) Au_{25} nanoclusters. Dotted lines represent energy upon an applied voltage of U = -1.0 V. * represents active site (S or Se atom).

References

1. M. Zhu, C. M. Aikens, F. J. Hollander, G. C. Schatz and R. Jin, *J. Am. Chem. Soc.*, 2008, **130**, 5883-5885.
2. G. Li, H. Abroshan, C. Liu, S. Zhuo, Z. Li, Y. Xie, H. J. Kim, N. L. Rosi and R. Jin, *Acs Nano*, 2016, **10**, 7998-8005.
3. Y. Song, J. Zhong, S. Yang, S. Wang, T. Cao, J. Zhang, P. Li, D. Hu, Y. Pei and M. Zhu, *Nanoscale*, 2014, **6**, 13977-13985.
4. J. P. Perdew, K. Burke and M. Ernzerhof, *Phys. Rev. Lett.*, 1996, **77**, 3865.
5. S. Goedecker, M. Teter and J. Hutter, *Phys. Rev. B*, 1996, **54**, 1703.
6. J. VandeVondele and J. Hutter, *J. Chem. Phys*, 2007, **127**, 114105.
7. J. VandeVondele, M. Krack, F. Mohamed, M. Parrinello, T. Chassaing and J. Hutter, *Comput. Phys. Commun.*, 2005, **167**, 103-128.
8. J. Akola, M. Walter, R. L. Whetten, H. Häkkinen and H. Grönbeck, *J. Am. Chem. Soc.*, 2008, **130**, 3756-3757.
9. Y. Song, J. Zhong, S. Yang, S. Wang, T. Cao, J. Zhang, P. Li, D. Hu, Y. Pei and M. Zhu, *Nanoscale*, 2014, **6**, 13977-13985.
10. R. Jin, C. Zeng, M. Zhou and Y. Chen, *Chem. Rev.*, 2016, **116**, 10346-10413.
11. G. Li and R. Jin, *Acc. Chem. Res.*, 2013, **46**, 1749-1758.
12. N. Austin, S. Zhao, J. R. McKone, R. Jin and G. Mpourmpakis, *Catal. Sci. Technol.*, 2018, **8**, 3795-3805.
13. D. R. Alfonso, D. Kauffman and C. Matranga, *J. Chem. Phys.*, 2016, **144**, 184705.
14. S. Zhao, N. Austin, M. Li, Y. Song, S. D. House, S. Bernhard, J. C. Yang, G. Mpourmpakis and R. Jin, *ACS catal.*, 2018, **8**, 4996-5001.
15. J. K. Nørskov, J. Rossmeisl, A. Logadottir, L. Lindqvist, J. R. Kitchin, T. Bligaard and H. Jónsson, *J. Phys. Chem. B*, 2004, **108**, 17886-17892.